Polymer Chemistry

ROYAL SOCIETY OF CHEMISTRY

COMMUNICATION

View Article Online
View Journal | View Issue

Cite this: *Polym. Chem.*, 2023, **14**, 4153

Received 22nd July 2023,
Accepted 2nd September 2023

DOI: 10.1039/d3py00857f

rsc.li/polymers

Tröger's base-containing fluorenone organic polymer for discriminative fluorescence sensing of sulfamethazine antibiotic at ppb level in the water medium†

Ananthu Shanmughan, Mini Ajith Nithasha, Binduja Mohan, Deivasigamani Umadevi* and Sankarasekaran Shanmugaraju *

A new Tröger's base containing fluorenone organic polymer (TB-FL-COP) was synthesized and used as a fluorescence sensor for discriminative sensing of antibiotics in water. TB-FL-COP showed the highest fluorescence quenching, reversible sensing responses, and excellent sensitivity of 56 ppb level for sulfamethazine antibiotics. The Stern–Volmer quenching constant (K_{SV}) was calculated to be 1.2 × 10^6 M^{-1}. The fluorescence sensing ability was also reflected by sharp visual color changes and further demonstrated in real water samples.

Introduction

Since their discovery in the early 20th century, antibiotics have been widely used to treat various bacterial infections in humans and animals.[1,2] The excess use and improper disposal have made antibiotics an emerging organic contaminant and hazardous environmental pollutant.[3] The large accumulation of antibiotics in waterbodies is a serious threat to human health and the ecosystem due to their wide dispersal, complex composition, and slow degradation.[4] Sulfonamides are a class of synthetic antibiotics with exceptional characteristics such as low-cost synthesis, good water solubility, rapid adsorption, and ease of transport.[5,6] Given their broad-spectrum activity and efficacy as a growth promoter, sulfonamide antibiotics are used in veterinary and animal husbandry.[7] Sulfamethazine (SMZ, 4-amino-*N*-(4,6-dimethyl-2-pyrimidinyl) benzene sulfonamide, is an essential antibiotic frequently used to treat and prevent antimicrobial and various protozoan infections.[8] SMZ is effective against chronic as well as acute bacterial infections in food-producing animals (cows, chickens, pigs, and so on).[9] It is also used against Gram-positive and Gram-negative bacteria.[10] The antibacterial property of SMZ emanates from their inhibition of *p*-aminobenzoic acid conversion, which interrupts folic acid synthesis and hence, restricts DNA replication.[11] Despite its effective bacteriostatic property, SMZ antibiotics do not completely metabolize in the living system.[12] Therefore, a large amount of SMZ antibiotic is excreted through urine or faeces and they can smoothly enter into the food chain through aquatic organisms and crops.[13] Besides, the excess antibiotic-based treatments applied to livestock led to the presence of antibiotic residues in the slaughtered meat and other animal products that are consumed by humans. This could eventually lead to the development of drug resistance in the intestinal bacterial population.[14] Furthermore, SMZ can cause severe allergic reactions as well as thyroid tumors in humans.[15] In response to these hazardous problems, various countries and international institutions have established regulations to control SMZ. The allowed limit of sulfonamide antibiotics in animal-origin foodstuffs is 100 ng g^{-1} by the European Union and China.[16] All these data alert the urgent need for an efficient sensing method for the trace detection of SMZ antibiotics.

Several instrumental techniques including Raman spectroscopy, capillary electrophoresis, and ion mobility spectrometry are currently used for the detection of antibiotics.[17,18] However, massive instrumentation setup, high-maintenance cost and tedious instrument calibration, and required trained technician impair their practical utilization.[19] On the other hand, fluorescence-based sensing has become an attractive method for trace analysis of antibiotics because of its high sensitivity, fast response time, and easy operational procedure.[20,21] Given this, in recent years, a wide variety of fluorescence sensors such as luminescent metal–organic frameworks, fluorescent organic polymers, and small-molecule fluorescent sensors have been developed and employed for the detection of different kinds of antibiotics.[1,22,23] Among the various fluorescence sensors known, luminescent covalent organic polymers (COPs) have become a popular sensor system

Department of Chemistry, Indian Institute of Technology Palakkad, Palakkad-678557, Kerala, India. E-mail: shanmugam@iitpkd.ac.in, umadevi@iitpkd.ac.in

†Electronic supplementary information (ESI) available: Solid-state CP-MAS ^{13}C-NMR, thermogravimetric analysis, powder X-ray diffraction pattern, gas adsorption isotherm and fluorescence studies. See DOI: **https://doi.org/10.1039/d3py00857f**

for antibiotics detection because of their facile synthesis, modular functional properties, amplified sensing responses, superior sensitivity to analytes, and high thermal and chemical stability.[24,25]

Considering these advantages, herein, we report a new Troger's base containing fluorenone luminescent organic polymer (**TB-FL-COP**) for fluorescence 'turn-off' sensing of antibiotics, in particular for selective, sensitive, quick, and reversible sensing of SMZ antibiotics in water. We introduced Tröger's base moiety because its unique V-shaped structure provides a large hydrophobic cavity that can be exploited for effective host–guest complexation with guest molecules.[26] The C_2 symmetry of Tröger's base bicyclic unit could easily be introduced within the polymer skeleton by a simple acid-catalyzed cyclization reaction of aromatic primary amines with paraformaldehyde or dimethoxymathane.[27–30] Tröger's base structure contains two stereogenic 'N' atoms which can act as potential receptor sites (Lewis base) for the recognition and sensing of various analytes.[31–33] Likewise, the π-electron-rich fluorenone moiety was introduced on the backbone of the polymer chain because of its rich-photophysical properties and diverse optoelectronic applications.[34,35] Also, the large aromatic surface of fluorenone endows the polymers to be highly emissive and can form an efficient donor–acceptor type complex with π-electron-deficient analytes through supramolecular interactions.[36]

Experimental section

Materials and methods

All reagents, solvents, and starting precursors were purchased from Sigma-Aldrich and were used as received. Commercially available reagent-grade chemicals were used for the synthesis of monomer and polymer **TB-FL-COP**. Spectroscopy-grade solvents purchased from Merck were used without further purification. 9-Fluorenone, aniline, aniline hydrochloride, dimethoxymethane, and trifluoroacetic acid (TFA) were purchased from Sigma-Aldrich and were used as received. The reagent-grade antibiotics analytes were purchased from Sigma-Aldrich and were used in sensing studies as purchased. Deuterated solvent $(CD_3)_2SO$ used for NMR analyses of monomer was purchased from Sigma-Aldrich. The monomer, 4,4′-(9*H*-fluorene-9,9-diyl)dianiline from 9-fluorenone, was synthesized following the procedure reported in the literature.[37]

The Shimadzu Scientific Instruments (IR Tracer 100) equipped with an ATR sampler were used to obtain the FT-IR spectrum of the polymer. The solid-state CP-MAS ^{13}C-NMR spectrum of **TB-FL-COP** was acquired at 201.1 MHz using a 3.2 mm double-resonance MAS probe. Thermogravimetric analysis (TGA) of **TB-FL-COP** was performed on the PerkinElmer STA 8000 analyzer equipped with an ultra-microbalance with a sensitivity of 0.1 mg. The temperature range was from 25 °C to 800 °C with a scan rate of 10 °C min^{-1} under the N_2 purge. The powder X-ray diffraction analysis was performed on Rigaku (XRD Smart Lab) diffractometer operating at 9 kW. The morphology of **TB-FL-COP** was imaged using field-emission scanning electron microscopy (FE-SEM) on Carl Zeiss (Gemini SEM 300) microscopy. The sample was prepared by drop-casting the suspension of the as-synthesized polymer on silica wafers, then coated with Au and dried under vacuum before the imaging.

The surface area of the polymer was determined using an N_2 physisorption isotherm. Before the adsorption measurement, the sample was evacuated under a vacuum to remove already trapped solvents. The UV-visible absorption spectra were recorded in a 1 cm quartz cuvette on a Thermo Fisher scientific spectrometer, and baseline correction was applied for all spectra. The emission spectra for all the experiments were recorded on a PerkinElmer FL-8500 fluorescence spectrophotometer equipped with a xenon arc (150 W) light source. The temperature was kept constant throughout the measurements at 298 K. All spectroscopic measurements were recorded in a quartz cuvette with a scan rate of 1200 nm min^{-1}. The obtained results were plotted using Origin Pro 8.5 software.

Synthesis of polymer TB-FL-COP

72.6 mg of 4,4′-(9*H*-fluorene-9,9-diyl)dianiline monomer was taken in a two-necked round-bottom flask and kept under stirring in an ice bath. 200 μL of dimethoxymethane (DMM) was added to the flask. N_2 was purged continuously into the flask to create an inert atmosphere. Then, 1 ml of TFA was added dropwise to the mixture using a syringe, and the reaction mixture was kept under stirring for 16 hours. A brown-colored liquid was obtained after the completion of the reaction and this liquid was added dropwise to the flask containing 10 mL of aqueous ammonia solution. After 2 hours of stirring a white-colored solid formed were separated from the solution. The white solid was filtered and washed with water (2 × 20 mL) followed by acetone (2 × 10 mL). The obtained white solid was dried under a vacuum and stored in a desiccator. The yield of the polymer **TB-FL-COP** was found to be 40% (calculated based on the monomer molecular weight). CP/MAS ^{13}C-NMR (solid-state): δ 34.00 (CH_2–Troger's base), 32.98 (CH_2–Troger's base); FT-IR (ATR, cm^{-1}): 3402, 3047, 2322, 1666, 1604, 1512, 1450, 1273, 1188, 1087, 933, 817, 740, 516.

Fluorescence sensing studies

2 mg of **TB-FL-COP** was dispersed in 10 mL of deionized water to prepare the stock solution. The sample was sonicated for 30 minutes and then aged for one day to obtain a uniformly dispersed solution. Similarly, a 1 mM stock solution of each of the antibiotics was freshly prepared in water. The 200 μL of stock solution of **TB-FL-COP** + 1800 μL of H_2O was taken in a 3 mL cuvette and then 1 mM stock solution of each of the antibiotics was added to the cuvette gradually and the emission intensity was recorded.

The percentage of fluorescence quenching efficiency was calculated from the following equation:

$$\text{Quenching efficiency } (\%) = (I_0 - I)/I_0 \times 100$$

where I_0 is the initial emission intensity of **TB-FL-COP** in water and I is the intensity after the addition of antibiotics.

The relative changes (I_0/I) in emission intensity upon increasing the concentration [Q] of antibiotics was demonstrated by the following Stern–Volmer equation:

$$I_0/I = K_{SV}[Q] + 1$$

The Stern–Volmer quenching constant (K_{SV}) was determined from the slope of the linear curve.

The limit of detection was calculated using the following equation:

$$\text{Limit of detection (LoD)} = 3\sigma/K$$

where σ is the standard deviation and K is the slope of the linear plot.

Results and discussion

Synthesis and characterization of TB-FL-COP

As shown in Scheme 1, Tröger's base-containing fluorenone organic polymer **TB-FL-COP** was synthesized by a simple acid-catalyzed one-pot cyclization reaction using the aromatic diamine, 4,4′-(9*H*-fluorene-9,9-diyl)dianiline, and dimethoxymethane in TFA under N_2 atmosphere at room temperature. The expected Tröger's base polymer **TB-FL-COP** was isolated as an off-white powder in 40% yield and found to be insoluble in most of the common organic solvents.[27]

The chemical structure of **TB-FL-COP** was characterized by FT-IR and solid-state cross-polarization magic-angle spinning (CP/MAS) ^{13}C NMR. In the FT-IR spectrum of **TB-FL-COP**, a new stretching band appeared at 1273 cm^{-1} corresponding to the C–N stretching vibrations of Tröger's base unit. Upon polymer formation, the intense broadband observed at 3348 cm^{-1} corresponding to the N–H stretching frequency of NH_2 groups of monomers nearly disappeared (Fig. 1A). In the CP-MAS ^{13}C-NMR spectrum, two peaks appeared at δ = 34.00 and 32.98 ppm corresponding to the C atoms of Tröger's base unit. These results strongly support the presence of Tröger's base moiety in the isolated **TB-FL-COP** polymer.

Thermogravimetric analysis (TGA) of **TB-FL-COP** under an N_2 atmosphere revealed that the as-synthesized polymer was stable up to 400 °C indicating its high thermal stability (Fig. S1, ESI†). The powder X-ray diffraction pattern of **TB-FL-COP** displayed a broad band with no obvious peaks which confirms the amorphous nature of **TB-FL-COP** (Fig. S2, ESI†). The amorphous form of **TB-FL-COP** facilitates its solution processability for sensing applications. The field-emission scanning electron microscopy (FESEM) imaging of **TB-FL-COP** showed that the polymer particles were aggregated to form a morphology of non-homogeneous sphere-shaped units on the solid surface (see Fig. 1B and C). The surface property of **TB-FL-COP** was evaluated using physisorption studies. Adsorption isotherm of N_2 intake was recorded at 77 K, which revealed that the **TB-FL-COP** has an average pore radius of 2.79 Å, and a pore volume of 0.571 cc g^{-1} (Fig. S3, ESI†). The Brunauer–Emmett–Teller (BET) surface area of the polymer was calculated to be 41 m^2 g^{-1} and hence, **TB-FL-COP** can be a potential molecular adsorbent for guest encapsulation.

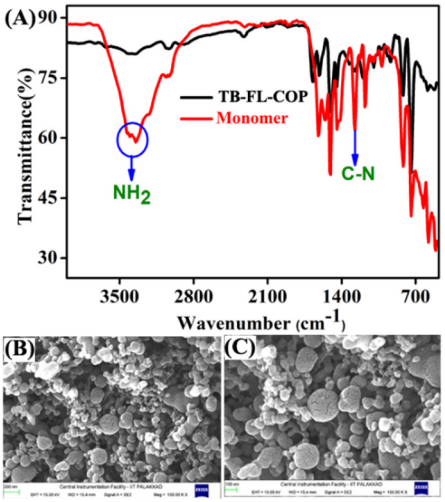

Fig. 1 (A) The FT-IR spectrum of polymer **TB-FL-COP** and monomer. The FESEM images of **TB-FL-COP** were imaged at (B) 100 and (C) 200 nm resolutions.

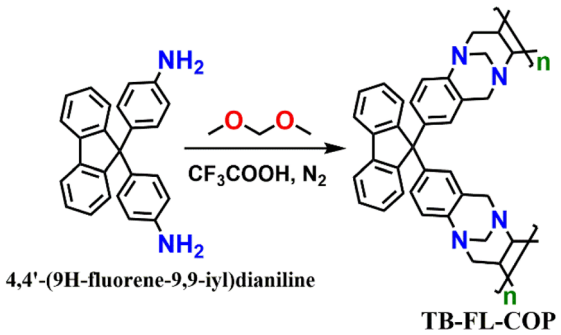

Scheme 1 The synthesis of polymer **TB-FL-COP**.

Fluorescence sensing of antibiotics

Having successfully synthesized and characterized, we then explored the fluorescence sensing properties of **TB-FL-COP** towards various antibiotics such as furazolidone (FZD), nitrofurazone (NFZ), chloramphenicol (CRP), nitrofurantoin (NFT), dimetridazole (DMZ), sulfamethazine (SMZ), and sulfadiazine (SDZ). Considering the practical use of polymer, all fluorescence sensing studies were performed in a water medium. The stock solution of **TB-FL-COP** was prepared by dispersing 2 mg in 10 mL of deionized water and 1.0×10^{-3} M stock solution of different antibiotics in deionized water was also prepared. To establish the sensing selectivity of **TB-FL-COP**, we first performed fluorescence titration studies using various antibiotics. The changes in fluorescence emission intensity of **TB-FL-COP** were measured before and after the addition of different antibiotics.

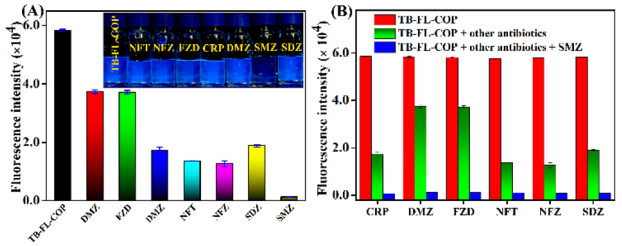

Fig. 2 (A) The extent of fluorescence quenching observed for **TB-FL-COP** after the addition of different antibiotics (Inset: observed visual color changes). (B) The relative changes in emission intensity of **TB-FL-COP** in the presence of various antibiotics along with or without SMZ antibiotics in the aqueous medium.

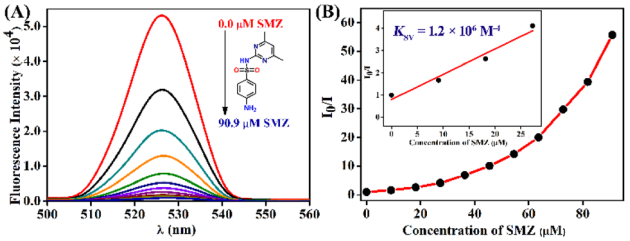

Fig. 3 (A) The observed changes in fluorescence emission intensity of **TB-FL-COP** at different concentrations of SMZ antibiotics and (B) corresponding Stern–Volmer plot (Inset: Stern–Volmer plot at low concentration of SMZ).

As shown in Fig. 2A, **TB-FL-COP** exhibited differential fluorescence quenching responses for different antibiotics. Among various antibiotics, SMZ antibiotics displayed the highest fluorescence quenching while other antibiotics such as FZD, CRP, NFT, DMZ, and SDZ showed moderate to poor fluorescence quenching responses. The high selectivity of **TB-FL-COP** for SMZ antibiotic was also reflected by a sharp visual color change (see Fig. 2A inset). The bright blue emission of **TB-FL-COP** become almost colorless upon the addition of SMZ while other antibiotics did not show any observable color changes. To further confirm the high selectivity of **TB-FL-COP** towards SMZ, competitive fluorescence titration studies were performed using SMZ in the presence of other competing antibiotics. As shown in Fig. 2B, the initial emission intensity of **TB-FL-COP** (red bar) was moderately quenched (green bar) upon the addition of various other antibiotics, however, the subsequent addition of SMZ antibiotic to the previous solution caused a strong fluorescence quenching (blue bar). These results demonstrate the preferential binding affinity and discriminative sensing propensity of **TB-FL-COP** towards SMZ even in the presence of other competing antibiotics.

To further probe the fluorescence sensing propensity of **TB-FL-COP** towards SMZ, a fluorescence titration study was carried out. The initial strong fluorescence emission at λ = 526 nm observed for **TB-FL-COP** was decreased in intensity upon the gradual increase in the concentration of SMZ (see Fig. 3A). From the fluorescence titration profile, a non-linear Stern–Volmer plot was obtained which indicates a complex fluorescence quenching mechanism involves in the overall quenching processes. The Stern–Volmer quenching constant $K_{SV} = 1.2 \times 10^6$ M^{-1} was determined from the slope of a linear plot obtained at a low concentration of SMZ. The relatively high K_{SV} value indicates a strong binding affinity of **TB-FL-COP** for SMZ antibiotics. The calculated K_{SV} value is comparable to other reported polymer-based fluorescence sensors for antibiotics.[38,39] Similar fluorescence titration studies in a PBS buffer medium using **TB-FL-COP** displayed a strong fluorescence quenching in the presence of SMZ and thus **TB-FL-COP** is a practically more useful sensor for SMZ detection (Fig. S4, ESI†). Likewise, under identical spectroscopic conditions, fluorescence titration was carried out using other antibiotics. It was observed that the extent of fluorescence quenching was different for different antibiotics and from the titration profile, the fluorescence quenching constant was calculated to be in the order of $K_{SV} = 10^3$–10^4 M^{-1}, these values are lower than the quenching constant calculated for SMZ (see Table S1 in ESI†).

Furthermore, the UV-visible absorption titration study and time-dependent fluorescence lifetime measurement were carried out to probe the plausible mechanism for the observed fluorescence quenching. As shown in Fig. S5 (in ESI†), the initial absorption intensity of **TB-FL-COP** increases with increasing the concentration of SMZ (0.0 to 90.9 × 10^{-6} M), which indicates that **TB-FL-COP** binds with SMZ in the ground-state. This was further supported by the time-dependent lifetime measurement. The lifetime of **TB-FL-COP** (τ = 0.1 ns) remained almost unchanged after the addition of SMZ antibiotics (90.9 × 10^{-6} M), except for a slight increase to 0.15 ns (Fig. S6 in ESI†). All these results including sharp visual color changes of **TB-FL-COP** after the addition of SMZ (Fig. 2A inset) and obtained linear Stern–Volmer plot at low concentration (Fig. 3B inset) indicate that **TB-FL-COP** forms a donor–acceptor type of charge-transfer (CT) complex with SMZ in the ground state at low concentration, which resulted in strong fluorescence quenching *via* the static quenching mechanism. However, a non-linear plot at a high concentration of SMZ indicates that fluorescence quenching is due to both static and dynamic quenching mechanisms (Fig. 3B).

The highest fluorescence quenching of **TB-FL-COP** for SMZ antibiotic was further validated by computational modeling using Density Functional Theory (DFT) calculations. All computational analyses were performed at the B3LYP/6-311++G(d,p) level of theory using the Gaussian 16 program.[40] The frontier molecular orbitals (HOMO and LUMO) energies for various antibiotics were calculated and compared with the HOMO and LUMO energy values of the **TB-FL-COP** model system. The LUMO energy value for antibiotics was found to be lower in energy than **TB-FL-COP** and thus, they can readily form a donor–acceptor type of charge transfer complex sensor and subsequently result in fluorescence quenching (see Table S2 in ESI†). The observed difference in the extent of fluorescence for different antibiotics is presumably due to the difference in the extent of energy transfer between the sensor and analyte. The

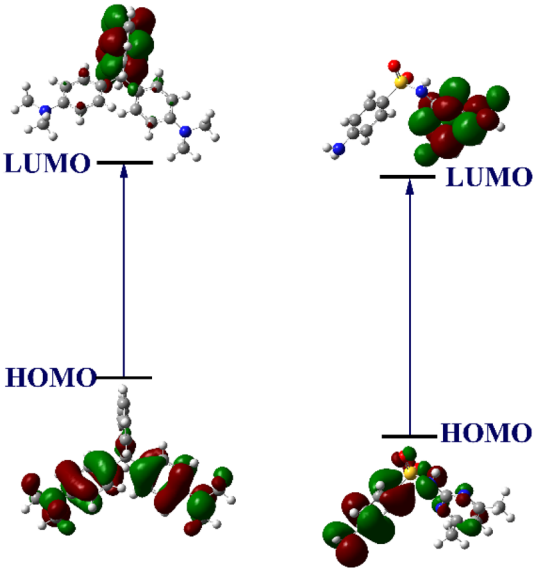

Fig. 4 The frontiers molecular orbitals (HOMO and LUMO) energy level diagram of **TB-FL-COP** and SMZ.

highest fluorescence quenching for SMZ was ascribed to its enhanced energy transfer from the sensor since the LUMO of SMZ is placed at lower energy and much closure to the LUMO of **TB-FL-COP** compared to the LUMO energy of all other antibiotics (Fig. 4).

To determine the sensitivity of **TB-FL-COP** for antibiotics detection, the fluorescence titration studies were performed by taking micromolar (μM) concentrations of SMZ. It was found that **TB-FL-COP** can detect the presence of SMZ even at the nanomolar (nm) level of concentrations and the LoD value was determined to be 56 ppb, this value of sensitivity is much lower than several other reported fluorescence and other types of sensors reported for antibiotic detection (see Table S3†).[41,42] A time-dependent fluorescence titration study was also performed to know the fluorescence quenching response time of **TB-FL-COP** for SMZ. The emission intensity of **TB-FL-COP** was monitored at various time intervals and quenching efficiency was plotted against contact time. Upon the addition of a 90.9 μM concentration of SMZ, a quenching efficiency of 98% was reached within 30 seconds after the addition of SMZ (Fig. S5A†). The instantaneous increase in fluorescence quenching indicates that **TB-FL-COP** can be used as a fast fluorescence sensor for antibiotics detection. Furthermore, the effect of the pH of the sensing medium on the sensing performances of **TB-FL-COP** towards SMZ was studied. As shown in Fig. S7 in ESI,† **TB-FL-COP** was found to be highly emissive in basic pH > 8 and the highest fluorescence emission was observed at pH = 10. While in the acidic pH < 5, **TB-FL-COP** was less emissive. Notably, the addition of SMZ antibiotics quenches the fluorescence emission of **TB-FL-COP** almost in all pH of the sensing medium. These results indicate that the effect of pH on the fluorescence sensing performance of **TB-FL-COP** is inconsequential.

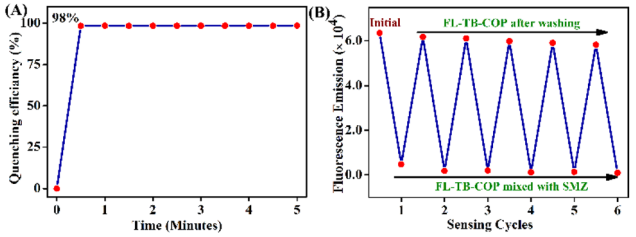

Fig. 5 (A) The percentage of fluorescence quenching was measured for **TB-FL-CP** after the addition of SMZ at a different time interval. (B) The reversible fluorescence sensing of **TB-FL-COP** for SMZ in water medium.

To check the reversibility, the fluorescent intensity of **TB-FL-COP** in water was measured before and after adding a 45.5 μM concentration of SMZ solution. After the measurement, the **TB-FL-COP** solution containing SMZ was washed several times with ethyl acetate to remove SMZ and subsequent fluorescence measurements indicate that **TB-FL-COP** regain the initial emission intensity. This procedure was repeated for several cycles and almost 91% of the initial emission intensity recovered even after six cycles. Thus, the recyclability of **TB-FL-COP** enriches its practical application of sensing antibiotics (see Fig. 5). To explore the sensor's usefulness in real-world applications, a fluorescence titration study with water samples was carried out. Water from a pond near Ahalia Hospital in Palakkad was used to make SMZ and **TB-FL-COP** stock solutions, which were then titrated to achieve high fluorescence quenching. Interestingly, **TB-FL-COP** exhibited a strong fluorescence quenching in the presence of SMZ in real-water samples (Fig. S8, ESI†). Despite the presence of many water contaminants and impurities in the pond water, the observed strong fluorescence quenching validates the potential application of **TB-FL-COP** for SMZ detection even in the real-water medium.

Conclusions

In conclusion, a new Tröger's base containing fluorenone organic polymer (**TB-FL-COP**) was developed and successfully used as a turn-off fluorescence sensor for the discriminative sensing of various antibiotics in an aqueous medium. Interestingly, **TB-FL-COP** showed a preferential binding affinity with the largest fluorescence quenching efficiency for sulfamethazine (SMZ) antibiotic and showed high selectivity, reversibility, and excellent sensitivity for SMZ detection. The selective sensing of SMZ antibiotic was also evident from the sharp visual color changes and thus **TB-FL-COP** can be a colorimetric probe. Further, we have demonstrated that **TB-FL-COP** can be employed to sense SMZ antibiotics in real-water samples. All the studies presented herein confirm that **TB-FL-COP** is a useful fluorescence sensor for selective, sensitive, and reversible sensing of SMZ antibiotics in water. As is given in Chart 1 (in ESI†), further works are in progress to explore the

applications of **TB-FL-COP** as a molecular filter for the efficient adsorption, removal, and conversion of different antibiotics from wastewater and device fabrications.

Author contributions

Ananthu Shanmughan: Data curation; formal Analysis; investigation; methodology; software; validation; writing – original draft. Mini Ajith Nithasha: Formal analysis; investigation; methodology; validation. Binduja Mohan: Data curation; investigation; writing – original draft. Deivasigamani Umadevi: Computational investigation and validation. Sankarasekaran Shanmugaraju: Conceptualization; funding acquisition; project administration; resources; supervision; validation; visualization; writing – original draft.

Conflicts of interest

There are no conflicts to declare.

Acknowledgements

The authors are grateful to the Indian Institute of Technology Palakkad (ERG research grant 2023-168-CHY-SHS-ERG-SP to SS), India, for financial support and CIF at the Indian Institute of Technology Palakkad for the facility.

References

1 P. R. Lakshmi, P. Nanjan, S. Kannan and S. Shanmugaraju, *Coord. Chem. Rev.*, 2021, **435**, 213793.
2 Q.-Q. Zhang, G.-G. Ying, C.-G. Pan, Y.-S. Liu and J.-L. Zhao, *Environ. Sci. Technol.*, 2015, **49**, 6772–6782.
3 R. Hirsch, T. Ternes, K. Haberer and K.-L. Kratz, *Sci. Total Environ.*, 1999, **225**, 109–118.
4 J. Zhang, Q. Sui, J. Tong, H. Zhong, Y. Wang, M. Chen and Y. Wei, *Environ. Int.*, 2018, **118**, 34–43.
5 R. Hirsch, T. Ternes, K. Haberer and K.-L. Kratz, *Sci. Total Environ.*, 1999, **225**, 109–118.
6 Z. Wang, K. Xing, N. Ding, S. Wang, G. Zhang and W. Lai, *J. Hazard. Mater.*, 2022, **423**, 127204.
7 Y. Liu and J. Wang, *J. Hazard. Mater.*, 2013, **250**, 99–105.
8 Q. Kou, P. Wu, Q. Sun, C. Li, L. Zhang, H. Shi, J. Wu, Y. Wang, X. Yan and T. Le, *Anal. Bioanal. Chem.*, 2021, **413**, 901–909.
9 Q.-Q. Zhang, G.-G. Ying, C.-G. Pan, Y.-S. Liu and J.-L. Zhao, *Environ. Sci. Technol.*, 2015, **49**, 6772–6782.
10 A. Feizollahi, A. A. Rafati, P. Assari and R. A. Joghani, *Anal. Methods*, 2021, **13**, 910–917.
11 B. Wang, X.-L. Lv, D. Feng, L.-H. Xie, J. Zhang, M. Li, Y. Xie, J.-R. Li and H.-C. Zhou, *J. Am. Chem. Soc.*, 2016, **138**, 6204–6216.
12 Y. Feng, J. Liu, D. Wu, Z. Zhou, Y. Deng, T. Zhang and K. Shih, *Chem. Eng. J.*, 2015, **280**, 514–524.
13 H. Dolliver, K. Kumar and S. Gupta, *J. Environ. Qual.*, 2007, **36**, 1224–1230.
14 S. W. Wright, K. D. Wrenn and M. L. R. N. Haynes, *J. Gen. Intern. Med.*, 1999, **14**, 606–609.
15 S. S. Amadei and V. Notario, *Antibiotics*, 2020, **9**, 580.
16 P. U. Wickramanayake, T. C. Tran, J. G. Hughes, M. Macka, N. Simpson and P. J. Marriott, *Electrophoresis*, 2006, **27**, 4069–4077.
17 A. L. Cinquina, F. Longo, G. Anastasi, L. Giannetti and R. Cozzani, *J. Chromatogr. A*, 2003, **987**, 227–233.
18 S. M. Ghoreishi, A. Khoobi, M. Behpour and S. Masoum, *Electrochim. Acta*, 2014, **130**, 271–278.
19 J. I. Lovitt, D. Umadevi, P. Raja Lakshmi, B. Twamley, T. Gunnlaugsson and S. Shanmugaraju, *Supramol. Chem.*, 2020, **32**, 620–633.
20 S. Shanmugaraju and P. S. Mukherjee, *Chem. Commun.*, 2015, **51**, 16014–16032.
21 S. Rojas and P. Horcajada, *Chem. Rev.*, 2020, **120**, 8378–8415.
22 T. Du, L. Huang, J. Wang, J. Sun, W. Zhang and J. Wang, *Trends Food Sci. Technol.*, 2021, **111**, 716.
23 A. Shanmughan, P. R. Lakshmi, D. Umadevi and S. Shanmugaraju, *Results Chem.*, 2022, **4**, 100546.
24 Q. Yang, H. Yu, Y. He, Z. Liu, C. Qin, B. Liu and Y. Li, *Eur. Polym. J.*, 2020, **123**, 109445.
25 J. Li, J. Liu, J. W. Y. Lam and B. Z. Tang, *RSC Adv.*, 2013, **3**, 8193–8196.
26 L. Mosca, J. Čejka, B. Dolenský, M. Havlík, M. Jakubek, R. Kaplánek, V. Král and P. Anzenbacher Jr., *Chem. Commun.*, 2016, **52**, 10664.
27 S. Shanmugaraju, D. Umadevi, A. J. Savyasachi, K. Byrne, M. Ruether, W. Schmitt, G. W. Watson and T. Gunnlaugsson, *J. Mater. Chem. A*, 2017, **5**, 25014; Q. Xu, B. Xin, J. Wei, Y. Ma, Z. Qing, C. Feng, S. Yi, N. Li, K. Li, F. Wang, J. Zhao, L. Yang, L. Yao, W. Jiang, Y. Dai and Z. Dai, *J. Mater. Chem. A*, 2023, **11**, 15600; M. Carta, R. Malpass-Evans, M. Croad, J. C. Jansen, P. Bernardo, F. Bazzarelli and N. B. McKeown, *Science*, 2013, **339**, 303–306.
28 A. F. M. EL-Mahdy, J. Lüder, M. G. Kotp and S.-W. Kuo, *Polymers*, 2021, **13**, 1385.
29 H. Hong, Z. Guo, D. Yan and H. Zhan, *Microporous Mesoporous Mater.*, 2020, **294**, 109870.
30 M. Carta, R. Malpass-Evans, M. Croad, Y. Rogan, M. Lee, I. Rosea and N. B. McKeown, *Polym. Chem.*, 2014, **5**, 5267.
31 Y. Cui, Y. Liu, J. Liu, J. Du, Y. Yu, S. Wang, Z. Liang and J. Yu, *Polym. Chem.*, 2017, **8**, 4842.
32 Z.-Z. Yang, H. Zhang, B. Yu, Y. Zhao, G. Jia and Z. Liu, *Chem. Commun.*, 2015, **51**, 1271.
33 C. Lin, Y. Gao, N. Li, M. Zhang, J. Luo, Y. Deng, L. Ling, Y. Zhang, F. Cheng and S. Zhang, *Electrochim. Acta*, 2020, **354**, 136693.
34 R. Abbel, A. P. H. J. Schenning and E. W. Meijer, *J. Polym. Sci., Part A: Polym. Chem.*, 2009, **47**, 4215.

35 N. Fomina and T. E. Hogen-Esch, *Macromolecules*, 2008, **41**, 3765.
36 M. Mandal and R. Balamurugan, *ChemistrySelect*, 2019, **4**, 10164.
37 X. Yan, H. Li, P. Shang, H. Liu, J. Liu, T. Zhang, G. Xing, Q. Fang and L. Chen, *Chem. Commun.*, 2021, **57**, 2136.
38 S. Wang, Q. Hu, Y. Liu, X. Meng, Y. Ye, X. Liu, X. Song and Z. Liang, *J. Hazard. Mater.*, 2020, **387**, 121949.
39 J.-M. Wang, X. Lian and B. Yan, *Inorg. Chem.*, 2019, **58**, 9956.
40 M. J. Frisch, G. W. Trucks, H. B. Schlegel, G. E. Scuseria, M. A. Robb, J. R. Cheeseman, G. Scalmani, V. Barone, G. A. Petersson, H. Nakatsuji, X. Li, M. Caricato, A. V. Marenich, J. Bloino, B. G. Janesko, R. Gomperts, B. Mennucci, H. P. Hratchian, J. V. Ortiz, A. F. Izmaylov, J. L. Sonnenberg, D. Williams-Young, F. Ding, F. Lipparini, F. Egidi, J. Goings, B. Peng, A. Petrone, T. Henderson, D. Ranasinghe, V. G. Zakrzewski, J. Gao, N. Rega, G. Zheng, W. Liang, M. Hada, M. Ehara, K. Toyota, R. Fukuda, J. Hasegawa, M. Ishida, T. Nakajima, Y. Honda, O. Kitao, H. Nakai, T. Vreven, K. Throssell, J. A. Montgomery Jr., J. E. Peralta, F. Ogliaro, M. J. Bearpark, J. J. Heyd, E. N. Brothers, K. N. Kudin, V. N. Staroverov, T. A. Keith, R. Kobayashi, J. Normand, K. Raghavachari, A. P. Rendell, J. C. Burant, S. S. Iyengar, J. Tomasi, M. Cossi, J. M. Millam, M. Klene, C. Adamo, R. Cammi, J. W. Ochterski, R. L. Martin, K. Morokuma, O. Farkas, J. B. Foresman and D. J. Fox, *Gaussian 16, Revision C.01*, Gaussian, Inc., Wallingford CT, 2016.
41 C. C. Shi, L. Zhao, X. Jia-Jia, L. Lu, A. Singh, O. Prakash and A. Kumar, *J. Inorg. Organomet. Polym. Mater.*, 2022, **32**, 4627.
42 K. Ren, S. H. Wu, X. F. Guo and H. Wang, *Inorg. Chem.*, 2019, **58**, 4223.